

**PASSIVE CONTROL OF SINGLE AND MULTIPLE JETS
USING CROSS WIRE VORTEX GENERATORS AT
SONIC AND SUPERSONIC MACH NUMBERS**

BY

MOHAMMED FAHEEM

A thesis submitted in fulfilment of the requirement for the
degree of Doctor of Philosophy (Engineering)

**Kulliyyah of Engineering
International Islamic University Malaysia**

DECEMBER 2021

ABSTRACT

The effectiveness of crosswire in controlling the mixing characteristics of a circular and an equivalent elliptic jet is investigated experimentally. While circular jets are conventional, elliptic jets have gained attention due to their better mixing characteristics and faster decay. To further explore and augment the capabilities of elliptic jets for practical utility, it is investigated whether using an elliptic jet with crosswire control gives additional benefit in mixing enhancement over an axisymmetric jet. Experiments are performed for subsonic and choked flow conditions with nozzle pressure ratios ranging from 1.2 to 7.0. Time-averaged pitot pressures and schlieren visualization is used for diagnosis. The jet bifurcation can be seen in controlled elliptical jets at all nozzle pressure ratios (NPRs). Core length is reduced to as much as 70% in the elliptic jet and 84% in the case of the circular jet. The core length values estimated from the present data are compared with the previous investigations. Mean flowfield and the mixing characteristics of free supersonic jets from twin and triple converging-diverging nozzles placed in proximity are also investigated. The nozzles are designed for Mach numbers 1.5 and 2.0, with an inter-nozzle spacing of twice the nozzle exit diameter. The typical interaction process and the evolution of the triple jet are discussed using cross-sectional contour plots. The influence of introducing additional similar jets on the near flowfield characteristics such as jet-spread, supersonic core, and the shock wave structure is studied using pressure measurements along the jet centerline. As the number of jets increases, the spreading rate decreases due to a reduction in the entrainment. This causes the jets to decay at a slow rate, and the core length increases in the order of an increased number of jets. Schlieren's images of single, twin, and triple jets reveal that the supersonic jet core is different in twin and triple when compared with a single plane. A simple yet effective approach is presented in the present work to get a reasonable estimate of the Mach number from the schlieren images for a Mach 2.0 nozzle jet. Results are compared with the numerical simulations for the estimated Mach number from the experimental data. The uncontrolled center line pitot pressure decay results obtained from numerical simulations are compared with the uncontrolled centerline pressure decay results obtained from the experimental. The crosswire tab is used as a passive control tool at the nozzle exit in two orientations to study the control effect. Schlieren's images reveal that the supersonic jet core is different in a controlled jet than the uncontrolled jet. Up to 83% reduction in core length is obtained from Mach 1.5 using vertical orientation of crosswire passive control at the nozzle ext. From the present research, it is evident that the crosswires' performance in multiple jets effectively reduces the supersonic core length at all NPRs of supersonic Mach numbers and higher NPRs of sonic Mach number. The most effective orientation in jet mixing enhancement is the vertical wire (control - 2) among the wire orientations studied.

خلاصة البحث

تم دراسة فعالية الأسلاك المتقاطعة في التحكم في خصائص الخلط لنفث إهليلجي دائري ومكافئ تجريبياً. في حين أن النفثات الدائرية تقليدية، فقد اكتسبت النفثات الإهليلجية الانتباه نظراً لخصائص الخلط الأفضل والأسرع في التحلل. لمزيد من استكشاف وزيادة قدرات النفثات الإهليلجية من أجل فائدة عملية، يتم التحقيق فيما إذا كان استخدام طائرة بيساوية مع التحكم في الأسلاك المتقاطعة يعطي فائدة إضافية في تحسين الخلط على نفث متماثل المحور. يتم إجراء التجارب لظروف التدفق دون سرعة الصوت والمختنق بنسب ضغط الفوهة تتراوح من 1.2 إلى 7.0. يتم استخدام ضغوط pitot بمتوسط الوقت والتصوير schlieren للتشخيص. يمكن رؤية التشعب النفث في نفثات بيساوية مضبوطة في جميع نسب ضغط الفوهة (NPRs). يتم تقليل طول النواة إلى ما يصل إلى 70% في النفث الإهليلجي و84% في حالة النفث الدائري. تتم مقارنة قيم الطول الأساسية المقدر من البيانات الحالية مع التحقيقات السابقة. يتم أيضاً فحص متوسط التدفق وخصائص الخلط للطائرات الأسرع من الصوت من النوزلات المتقاربة المزدوجة والثلاثية المتقاربة الموضوعية على مقربة. تم تصميم الفوهات لأعداد Mach 1.5 و 2.0 ، مع تباعد بين الفوهة ضعف قطر مخرج الفوهة. تتم مناقشة عملية التفاعل النموذجية وتطور الطائرة النفثة الثلاثية باستخدام مخططات كفاف مقطعية. تمت دراسة تأثير إدخال نفثات إضافية مماثلة على خصائص حقل التدفق القريب مثل الانتشار النفث ، واللب الأسرع من الصوت ، وهيكل موجة الصدمة باستخدام قياسات الضغط على طول خط الوسط النفث. مع زيادة عدد النفثات ، ينخفض معدل الانتشار بسبب انخفاض السحب. هذا يتسبب في تحلل النفثات بمعدل بطيء ، ويزيد طول النواة في ترتيب عدد متزايد من الطائرات. تكشف صور Schlieren للطائرات الفردية والثنائية والثلاثية أن قلب الطائرة الأسرع من الصوت يختلف في التوأم والثلاثي عند مقارنته بطائرة واحدة. تم تقديم نهج بسيط ولكنه فعال في العمل الحالي للحصول على تقدير معقول لعدد Mach من صور schlieren لنفث Mach 2.0. تمت مقارنة النتائج مع المحاكاة العددية لعدد الماخ المقدر من البيانات التجريبية. تمت مقارنة نتائج اضمحلال ضغط البيوتوت لخط الوسط غير المتحكم فيه التي تم الحصول عليها من عمليات المحاكاة العددية مع نتائج انحلال ضغط الخط المركزي غير المنضبط التي تم الحصول عليها من التجربة. يتم استخدام علامة تبويب الأسلاك المتقاطعة كأداة تحكم سلبية عند مخرج الفوهة في اتجاهين لدراسة تأثير التحكم. تكشف صور شليرين أن النواة النفثة الأسرع من الصوت تختلف في طائرة نفثة خاضعة للرقابة عن نفثة غير مسيطر عليها. يتم الحصول على تخفيض يصل إلى 83% في الطول المركزي من Mach 1.5 باستخدام التوجيه الرأسي للتحكم السلبي في الأسلاك المتقاطعة عند تحويل الفوهة. من البحث الحالي ، من الواضح أن أداء الأسلاك المتقاطعة في نفثات متعددة يقل بشكل فعال من طول النواة الأسرع من الصوت في جميع NPRs لأرقام ماخ الأسرع من الصوت وأعلى NPR من عدد ماخ الصوتي. الاتجاه الأكثر فاعلية في تحسين الخلط النفث هو السلك العمودي (التحكم - 2) بين اتجاهات الأسلاك المدروسة.

APPROVAL PAGE

The thesis of Mohammed Faheem has been approved by the following:



Sher Afghan Khan
Supervisor



Waqar Asrar
Co-supervisor



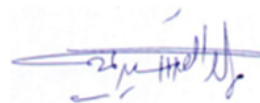
Mohd Azan bin Mohammed Sapardi
Co-supervisor



Erwin Sulaeman
Internal Examiner



Andrew Ragai Henry Rigit
External Examiner



Mohamed Elwathig Saeed Mirghani
Chairman

DECLARATION

I hereby declare that this thesis is the result of my own investigations, except where otherwise stated. I also declare that it has not been previously or concurrently submitted as a whole for any other degrees at IIUM or other institutions.

Mohammed Faheem

Handwritten signature of Mohammed Faheem in black ink, written in a cursive style.

Signature

Date : 07/12/2021

INTERNATIONAL ISLAMIC UNIVERSITY MALAYSIA

**DECLARATION OF COPYRIGHT AND AFFIRMATION OF
FAIR USE OF UNPUBLISHED RESEARCH**

**PASSIVE CONTROL OF SINGLE AND MULTIPLE JETS USING
CROSS WIRE VORTEX GENERATORS AT SONIC AND
SUPERSONIC MACH NUMBERS**

I declare that the copyright holders of this dissertation are jointly owned by the student and IIUM.

Copyright © thesis 2021 Mohammed Faheem and International Islamic University Malaysia. All rights reserved.

No part of this unpublished research may be reproduced, stored in a retrieval system, or transmitted, in any form or by any means, electronic, mechanical, photocopying, recording or otherwise without prior written permission of the copyright holder except as provided below

1. Any material contained in or derived from this unpublished research may be used by others in their writing with due acknowledgement.
2. IIUM or its library will have the right to make and transmit copies (print or electronic) for institutional and academic purposes.
3. The IIUM library will have the right to make, store in a retrieved system and supply copies of this unpublished research if requested by other universities and research libraries.

By signing this form, I acknowledged that I have read and understand the IIUM Intellectual Property Right and Commercialization policy.

Affirmed by Mohammed Faheem



.....

Signature

07/12/2021

.....

Date

ACKNOWLEDGEMENTS

In the Name of Allah, the Most Compassionate, the Most Merciful

Allah - beginning with the name of - the Most Gracious, the Most Merciful Most Auspicious is he in whose control is the entire kingship, and he can do all things [67:1]. All Praise to Allah, the Lord of the creation, and countless blessings and peace upon our Master Mohammed, the leader of the Prophets (peace be upon Him).

Firstly, it gives me great pleasure to dedicate this work to my dear parents, elder brother, sisters, my wife, and daughter, who have given me the gift of unwavering faith in my ability to achieve this goal: thank you for your support and patience.

My heartfelt thanks go to my advisor, Professor Dr. Sher Afghan Khan, who expertly guided me through my graduate studies. His unwavering enthusiasm for research kept me always interested, and his generosity contributed to my enjoyment of my time at IIUM.

Apart from my advisor, I'd like to thank my co-supervisors, Professor Dr. Waqar Asrar and Dr. Mohammed Azan bin Mohammed Sapardi, for their time, effort, encouragement, insightful comments, and support for this research study.

My wholehearted gratitude also goes to the Indian Institute of Technology, Kanpur, India, for their efforts and collaborative attitude in making this project a success, particularly Dr. Rakesh Kumar. M, assistant professor in the department of aerospace engineering, Mr. Aqib Khan, research scholar in the department of aerospace engineering, and Mr. Sunil Mishra, in charge of the IITK aerodynamic lab.

Finally, my thanks are also extended to the Dean, Deputy Dean-PG, Professor and Head, PG Coordinator of Mechanical Engineering Department, Kulliyah of Engineering faculty members, every member of the Centre of Postgraduate Studies, and the office of international affairs, who all contributed directly or indirectly to the successful completion of my research work.

TABLE OF CONTENTS

Abstract.....	ii
Abstract in Arabic.....	iii
Approval Page.....	iv
Declaration.....	v
Copyright Page.....	vi
Acknowledgements.....	vii
Table of Contents.....	viii
List of Tables.....	xi
List of Figures.....	xii
List of Symbols.....	xvii
List of Abbreviations.....	xviii
CHAPTER ONE : INTRODUCTION.....	1
1.1 Background of the Study.....	1
1.1.1 Jets.....	1
1.1.2 Jet Mixing.....	3
1.1.3 Development of Axi-symmetric Supersonic Jets.....	5
1.1.4 Jet Decay.....	7
1.1.5 Jet Control.....	8
1.1.6 Types of Jet Control.....	8
1.1.6.1 Active Control.....	8
1.1.6.2 Passive Control.....	9
1.1.7 Flowfield of Multiple Jets.....	9
1.2 Statement of the Problem.....	10
1.3 Research Objectives.....	11
1.4 Research Philosophy.....	11
1.5 Research Methodology.....	12
1.6 Research Scope.....	14
1.7 Limitations of the Study.....	14
1.8 Thesis Outline.....	15
CHAPTER TWO : LITERATURE REVIEW.....	16
2.1 Introduction.....	16
2.2 Vortical Structures.....	17
2.3 Tabs.....	23
2.4 Free Jet Morphology.....	28
2.5 Calculation of supersonic core length.....	28
2.6 Elliptical Jets.....	30
2.7 Effect of Crosswires on Vorticity Dynamics.....	32
2.8 Introduction to Multiple Nozzles.....	35
2.9 Co-flowing Jets.....	38
2.10 Mach Number Estimation.....	39
2.11 Applications of Jet Control.....	41
2.11.1.1 Infra-red Signature Reduction.....	41

2.11.1.2	Supersonic Combustion.....	41
2.11.1.3	Combustion Systems.....	42
2.11.1.4	Jet Noise Reduction.....	42
2.11.1.5	Ejectors.....	43
2.11.1.6	Metal Deposition.....	43
2.11.1.7	Thrust Vector Control.....	44
2.11.1.8	Base Heat Reduction in the Case of Launch Vehicles.....	44
2.11.1.9	Basic Oxygen Process of Steelmaking.....	44
2.11.1.10	Convergent-divergent (CD) Nozzle.....	45
2.12	Summary.....	46

CHAPTER THREE : EXPERIMENTAL SETUP AND PROCEDURE 47

3.1	Experimental Setup.....	47
3.1.1	Jet Flow Facility.....	47
3.2	Data Acquisition.....	49
3.2.1	Instrumentation and Data Accuracy.....	49
3.3	Experimental Model.....	51
3.3.1	Sonic Nozzle.....	51
3.3.2	Supersonic Nozzle.....	53
3.3.3	Nozzle Calibration.....	56
3.3.4	Test Metrics.....	56
3.4	Experimental Procedure.....	57
3.4.1	Setting up the Nozzle Test Rig.....	58
3.4.2	Setting up the Visualization System.....	59
3.4.3	Performing the Test.....	59
3.4.4	Post-test Actions.....	60
3.4.5	Coordinate System Used in the Experiment.....	61
3.4.6	Centerline Pressure Decay.....	62
3.4.7	Pressure Profile Plots.....	63
3.4.8	Flow Visualization.....	64
3.4.9	Calculation of Supersonic Core Length.....	66
3.4.10	Data Accuracy.....	66
3.4.11	Precautions Observed.....	66
3.5	Error Analysis.....	67
3.5.1	Uncertainty Analysis.....	68
3.5.2	Uncertainty in Flow Mach Number (XMe).....	69
3.5.3	Uncertainty in Nozzle Pressure Ratio (X_{NPR}).....	70
3.5.4	Uncertainty in Core Length (XLc).....	71
3.5.5	Uncertainty in Percentage Reduction in Core Length ($X_{\Delta Lc}$).....	72
3.6	Calculation of Reynolds Number.....	72
3.7	Nozzle Design.....	73

CHAPTER FOUR : RESULTS AND DISCUSSIONS 75

4.1	Sonic Mach Number.....	75
4.1.1	Control of Subsonic Jet.....	75
4.1.1.1	Centerline Pitot Pressure Decay of Subsonic Jet.....	75
4.1.2	Control of Underexpanded Jet.....	77
4.1.2.1	Nozzle Pressure Ratio 2.....	77
4.1.2.2	Nozzle Pressure Ratio 3.....	79

4.1.2.3	Nozzle Pressure Ratio 4	82
4.1.2.4	Nozzle Pressure Ratio 6	83
4.1.2.5	Nozzle Pressure Ratio 7	84
4.1.3	Transverse Pressure Profiles of Sonic Jet.....	86
4.1.4	Supersonic Core Length and Shock Cell Characteristics	88
4.2	Supersonic Mach Number – Uncontrolled.....	93
4.2.1	Flowfield Evolution of Triple Jet.....	93
4.2.2	Centerline Pressure Profiles for Single and Multiple Jets	100
4.2.3	Supersonic Core Length and Shock Cell Characteristics	106
4.3	Supersonic Mach Number – Controlled	114
4.3.1	Centerline Pressure Profiles for Single and Multiple Jets	115
4.3.1.1	CPD of Mach 1.5	115
4.3.1.2	CPD of Mach 2.0	122
4.3.2	Transverse Pressure Profiles of Supersonic Jet	129
4.3.3	Midplane Jet Evolution (CenterLine).....	137
4.3.4	Midplane Jet Evolution (Centroid).....	139
4.3.5	Isobaric Pressure Contours	139
4.3.5.1	Twin Jet	139
4.3.5.2	Triple Jet.....	143
4.3.6	Flow Visualization	146
4.3.6.1	Single Jet	146
4.3.6.2	Twin Jet	148
4.3.6.3	Triple Jet.....	152
4.4	Numerical Analysis.....	160
4.4.1	Simulation Details.....	160
4.5	Summary	167
CHAPTER FIVE : CONCLUSIONS		168
5.1	Conclusions	168
5.2	Future Scope.....	170
REFERENCES		171
LIST OF PUBLICATIONS.....		183
Journal Articles		183
Conference Proceedings		184

LIST OF TABLES

Table 3.1	Test metrics of circular sonic jet	57
Table 3.2	Test metrics of supersonic jet	57
Table 4. 1	Sonic point pressure ratio for the estimation of supersonic core length	89
Table 4.2	Identification of data points for supersonic circular jet core-length and comparison of results with the previous studies	90
Table 4.3	Core length and % change in core length of the jets at different NPRs	91
Table 4.4	Supersonic core-length of single, twin, and triple jet by the method discussed in Ref (Perumal & Rathakrishnan, 2014)	110
Table 4.5	Shock-cell lengths for single jet	113
Table 4.6	Shock-cell lengths for single and multiple jets	113
Table 4.7	Core length and percentage change in core length of the jets for Mach 1.5	122
Table 4.8	Core length and percentage change in core length of the jets for Mach 2.0	129

LIST OF FIGURES

Figure 1.1	Sideview of the jet development. The arrow implies a streamwise structure at $x / d = 3.5$ (Liepmann & Gharib, 1992).	2
Figure 1.2	Diagrammatic presentation of the different zones in developing a subsonic jet (E. Rathakrishnan, 2010).	3
Figure 1.3	Classification of jets (E. Rathakrishnan, 2010)	6
Figure 1.4	Flowchart of research method.	13
Figure 1.5	Schematic illustration of the screech tone feedback loop (Christopher K. W. Tam, 1995).	41
Figure 2. 1	Illustration of subsonic potential core and supersonic core length (Faheem, Khan, Kumar, Khan, et al., 2021)	29
Figure 2.2	Schematic of flow at the nozzle exit demonstrating the distribution of vortices at the nozzle wall and along the crosswire. The controlled cases are drawn with crosswire size exaggerated for representation purposes.	34
Figure 3.1	Schematic diagram of the jet facility	48
Figure 3.2	Open jet facility of high-speed aerodynamics laboratory (Akram & Rathakrishnan, 2019).	49
Figure 3.3	Outline of high-speed aerodynamics laboratory.	49
Figure 3.4	16-channel Pressure Systems, Inc.9010 transducer (Akram & Rathakrishnan, 2019)	51
Figure 3.5	Dimensions of the sonic elliptic nozzle and wire orientation at the exit $2d$ (All dimensions are in mm).	52
Figure 3.6	Dimensions of elliptical and circular sonic nozzle blocks $2d$ (All dimensions are in mm).	53
Figure 3.7	Mach 2.0 nozzle block and dimensions $2d$ (All dimensions are in mm).	54
Figure 3.8	Machined model of Mach 1.5 nozzle block with control orientations.	55
Figure 3.9	Dimensions of nozzle block for Mach 1.5 with internozzle spacing $2d$ $2d$ (All dimensions are in mm).	55

Figure 3.10	Dimensions of nozzle block for Mach 2.0 with internozzle spacing $2d$ (All dimensions are in mm).	55
Figure 3.11	Illustration of coordinate axes and transverse data acquisition location. Lines in Y-axis show the location of transverse data measurement.	61
Figure 3.12	Illustration of coordinate axes and contour data acquisition location. Planes show the location of contour data measurement.	62
Figure 3.13	Measurement stencil showing an axial increment of the jet.	63
Figure 3.14	Schematic of the pitot pressure measurement normal to the tabs	64
Figure 3.15	Schematic of schlieren setup	65
Figure 3.16	Postprocessing of the schlieren image.	65
Figure 4.2	Centerline pressure decay of elliptical and circular jets at different NPRs	76
Figure 4.3	Flow visualization of elliptical jets at NPR 2	78
Figure 4.4	Centerline pressure decay of elliptical and circular jets at NPR 2	78
Figure 4.5	Flow visualization of elliptical jets at NPR 3	80
Figure 4.6	Centerline pressure decay of elliptical and circular jets at NPR 3	80
Figure 4.7	Flow visualization of elliptical jets at NPR 4	83
Figure 4.8	Centerline pressure decay of elliptical and circular jets at NPR 4	83
Figure 4.9	Flow visualization of elliptical jets at NPR 6	83
Figure 4.10	Centerline pressure decay of elliptical and circular jets at NPR 6	84
Figure 4.11	Flow visualization of elliptical jets at NPR 7	85
Figure 4.12	Centerline pressure decay of elliptical and circular jets at NPR 7	85
Figure 4.13	Transverse pressure profiles of the elliptical jet at NPR 3.0 and 6.0	87
Figure 4.14	Transverse pressure profiles of the circular jet at NPR 3.0 and 6.0	88
Figure 4.16	Comparison of measured and visual flowfield for the elliptical jet at NPR 4	89
Figure 4.17	Percentage change in core length with an expansion ratio	92

Figure 4.18	Illustration of coordinate axes and contour data acquisition location.	93
Figure 4.19	Isobaric pressure contours for NPR = 3 at Mach number 1.5	95
Figure 4.20	Transverse pressure profile for Mach 1.5 single and twin jet at NPR of 3	97
Figure 4.21	Transverse pressure profile for Mach 1.5 single and twin jet at NPR of 5	98
Figure 4.22	Evolution of the jet in the internozzle region. Figures on the left side (a and c) show the variation of pressure in the internozzle region for M 1.5 and 2.0 triple jet, whereas figures on the right side (b and d) show the fractional change in the pressure values to emphasize the influence of the mutual interaction of three jets on the flowfield in the internozzle region.	99
Figure 4.23	Centerline pressure decay for Mach number 1.5 jet for different NPRs	101
Figure 4.24	Centerline pressure decay for Mach number 2.0 jet for different NPRs	104
Figure 4.25	Evolution of the jet in the internozzle region for Mach 1.5 and 2.0 jets. Single corresponds to the case when only one nozzle is operational while the other two are mute-like twin and triple corresponds to two and three nozzles under operation, respectively.	105
Figure 4.26	Comparison of measured and visual flowfield for the single jet at Mach number 1.5 for NPR of 7	107
Figure 4.27	Schlieren image of Mach 1.5 single, twin, and triple jet. Flow is from left to right.	108
Figure 4.28	Percentage change in core length for Mach 1.5 and 2.0	110
Figure 4.29	CPD for Mach number 1.5 at overexpanded NPR = 2.	116
Figure 4.30	CPD for Mach number 1.5 at overexpanded NPR = 3.	118
Figure 4.31	CPD for Mach number 1.5 at correctly expanded NPR = 3.67.	119
Figure 4.32	CPD for Mach number 1.5 at underexpanded NPR = 5.	120
Figure 4.33	CPD for Mach number 1.5 at underexpanded NPR = 7.	122
Figure 4.34	CPD for Mach number 2.0 at overexpanded NPR = 2.	123
Figure 4.35	CPD for Mach number 2.0 at overexpanded NPR = 4.	125

Figure 4.36	CPD for Mach number 2.0 at overexpanded NPR = 6.	126
Figure 4.37	CPD for Mach number 2.0 at correctly expanded NPR = 7.82.	127
Figure 4.38	CPD for Mach number 2.0 at underexpanded NPR = 8.5.	128
Figure 4.39	Transverse pressure profiles of Mach 1.5 single and twin jet at NPR = 3.0.	133
Figure 4.40	Transverse pressure profiles of Mach 1.5 single and twin jet at NPR = 3.67.	133
Figure 4.41	Transverse pressure profiles of Mach 1.5 single and twin jet at NPR = 5.0.	134
Figure 4.42	Transverse pressure profiles of Mach 2.0 single and twin jet at NPR = 4.0.	135
Figure 4.43	Transverse pressure profiles of Mach 2 single and twin jet at NPR = 7.82	136
Figure 4.44	Transverse pressure profiles of Mach 2.0 single and twin jet at NPR = 8.5.	136
Figure 4.45	Jet evolution at the internozzle region (midpoint of two jets) of twin jet and triple jet for Mach 2.0 at various NPRs.	138
Figure 4.46	Jet evolution at the internozzle region (center of three jets) of the triple jet at Mach 2.0	139
Figure 4. 47	Isobaric pressure contours of twin jet with control 1 (horizontal wire) at Mach 1.5	141
Figure 4.48	Isobaric pressure contours of twin jet with control 2 (vertical wire) at Mach 1.5	141
Figure 4. 49	Isobaric pressure contours of twin jet with control 1 (horizontal wire) at Mach 2.0	142
Figure 4.50	Isobaric pressure contours of twin jet with control 2 (vertical wire) at Mach 2.0	142
Figure 4.51	Isobaric pressure contours of triple jet with control - 1 (horizontal wire) at Mach 1.5	144
Figure 4.52	Isobaric pressure contours of triple jet with control - 2 (vertical wire) at Mach 1.5	145
Figure 4.53	Isobaric pressure contours of triple jet with control - 1 (horizontal wire) at Mach 2.0	145

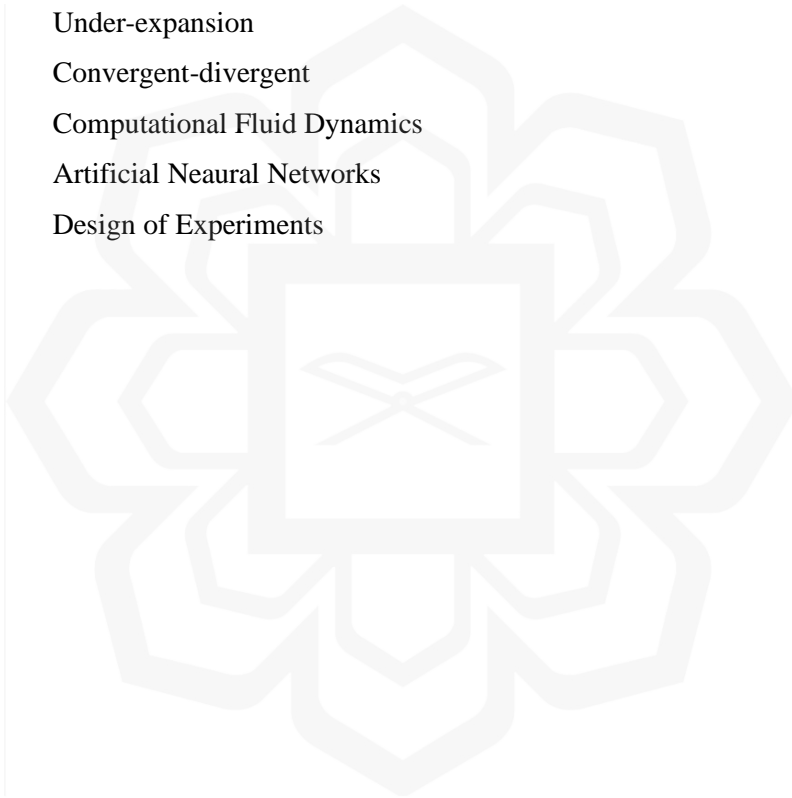
Figure 4.54	Isobaric pressure contours of triple jet with control - 2 (vertical wire) at Mach 2.0	146
Figure 4.55	Schlieren image of Mach 1.5 single jet at different NPRs	147
Figure 4.56	Schlieren image of Mach 2.0 single jet at different NPRs	148
Figure 4.57	Schematic of the direction of flow visualization during schlieren for twin jet.	150
Figure 4.58	Schlieren image of Mach 1.5 twinjet at different NPRs	151
Figure 4.59	Schlieren image of Mach 2.0 twinjet at different NPRs	152
Figure 4.60	Schematic of the direction of flow visualization during schlieren for the triple jet.	153
Figure 4.61	Schlieren images of Mach 1.5 triple jet at different NPRs	158
Figure 4.62	Schlieren images of Mach 2.0 triple jet at different NPRs	159
Figure 4.63	Picture of final mesh used for simulation.	160
Figure 4.64	Grid independency test.	161
Figure4.65	Centerline pitot pressure decay different NPRs and corresponding pressure expansion of M2.0 single jet	164
Figure 4.66	Wave structure in the jet from the numerical simulation.	165
Figure 4.67	Mach number variation along the jet centerline.	166
Figure 4.68	Comparison of experimental and numerical centerline pitot pressure decay at various NPRs for Mach 1.5	166
Figure 4.69	Comparison of experimental and numerical centerline pitot pressure decay at various NPRs for Mach 2.0	167

LIST OF SYMBOLS

M/M_d	Design Mach number
M_c	Convective Mach number
M_j	Jet exit Mach number
$P_{atm} = P_a = P_b$	Static atmospheric pressure = Static ambient pressure = Backpressure
P_t	Pressure measured by pitot tube
P_0	Stagnation pressure of the settling chamber
P_e	Pressure at the exit plane of the nozzle
n	Static pressure ratio at the nozzle exit (P_e / P_a)
d	Nozzle exit diameter
d^*	Throat diameter
A_e	Area at nozzle exit
A^*	Area at the throat
U_j	Jet exit velocity
L_c	Supersonic core length
ΔL_c	Percentage core length reduction
L_s	Shock cell spacing
Re_j	Reynolds number of the jet at exit
γ	Ratio of specific heats
x	Coordinate along the jet axis
y	Coordinate normal to the horizontal wire (Transverse)
z	Coordinate normal to the vertical wire
T_0	Stagnant temperature
a	Speed of sound

LIST OF ABBREVIATIONS

CPD	Centerline pitot pressure decay
HW	Horizontal wire
VW	Vertical wire
NPR	Nozzle pressure ratio $(P_0 / P_{atm}) = (P_0 / P_a)$
OE	Overexpansion
CE	Correct expansion
UE	Under-expansion
CD	Convergent-divergent
CFD	Computational Fluid Dynamics
ANN	Artificial Neural Networks
DOE	Design of Experiments



CHAPTER ONE

INTRODUCTION

1.1 BACKGROUND OF THE STUDY

For many years, flow via nozzles has been examined in various configurations. Nozzle flows with air and water as fluids have been extensively researched, owing to their ease of availability and widespread applicability. The flow property changes associated with nozzle flow have always sparked the scientific and engineering communities' curiosity. The flow regimes and attributes of simple converging and diverging nozzles have been thoroughly studied during the past many years. The introduction of jet engines and their subsequent use as propulsive units for aircraft accelerated the research. However, because of their well-defined, homogeneous jet development, circular nozzles were first the focus of the research. Aside from that, the ease with which it could be manufactured and incorporated into the gas turbine engines used by its host aircraft meant that it was preferred over other types of nozzles. This chapter caters to the importance of the jets, characteristics of jets, and their applications. The aim is to provide the background and motivations for undertaking the contemporary study, which catalyzes the rest of the thesis. Section 1.1 presents the background about nozzle flow.

1.1.1 Jets

A free jet is characterized as a pressure-driven shear flow that, upon exiting the nozzle, has the property that the width-to-axial distance (x / d ; where x is any axial position and 'd' is the local diameter of the jet) is constant (Abramovich, 2020). For jet Mach number of 0.2, this constant maintains a value of 8, and the constant

decreases as the Mach number increases, because when the Mach number increases compressibility comes into the picture, hence the constant decreases (E. Rathakrishnan, 2010).

The free shear layer is propelled by the momentum generated at the nozzle exit (Namer & Otugen, 1988). Due to initial instabilities, the shear layer tends to roll up and disrupt to form vortices as it exits the nozzle (Figure 1.1).

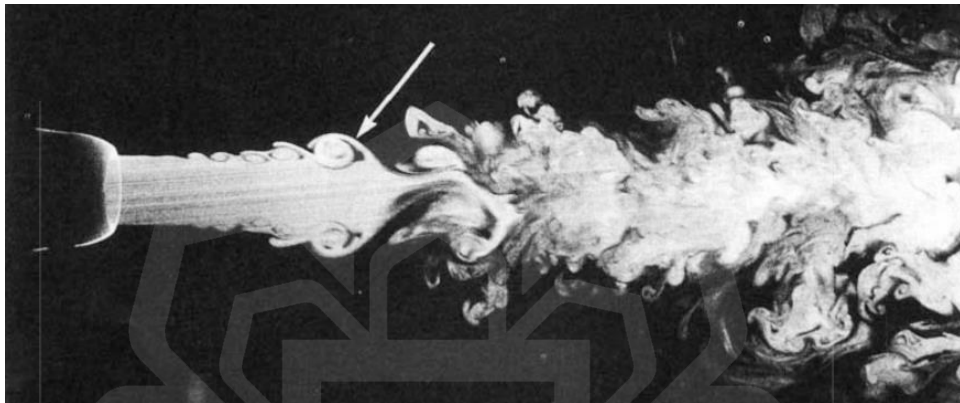


Figure 1.1 Sideview of the jet development. The arrow implies a streamwise structure at $x / d = 3.5$ (Liepmann & Gharib, 1992).

These vortices transport the surrounding fluid into the jet, causing mixing. As a result, mass flow increases gradually downstream at every cross-section of the jet. The ambient fluid momentum is less than that of the fluid elements in a jet emitted by a nozzle or orifice. As a result, the fluid masses with higher and lower momentum will attempt to achieve an equilibrium, resulting in a decrease in the jet mass's momentum released from the nozzle as it propagates downstream. Consequently, the vortices increase in size as they travel downstream, and the jet stretches sideways as the mixing regions thicken. Therefore, a finite-thickness area with a constant velocity distribution forms the boundary between the two jets; this region is known as the jet boundary layer. The mixing area is broad enough to penetrate the jet's centerline at some distance from the nozzle exit plane. So far, the mixing has not affected the

centerline velocity, which remains equivalent to the jet exit velocity. Hence, the region enclosed by the two mixing zones with no velocity gradient is the potential core. In other words, the region where mixing initiated at the jet boundaries has not yet breached the entire flow area, leaving a region with a constant axis velocity close to the jet exit velocity (Sforza et al., 1966). Figure 1.2 displays a line representation of the growth of a subsonic jet.

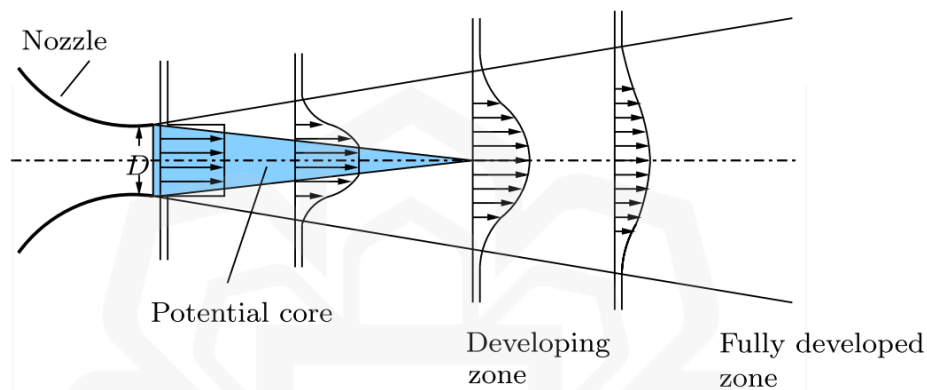


Figure 1.2 Diagrammatic presentation of the different zones in developing a subsonic jet (E. Rathakrishnan, 2010).

1.1.2 Jet Mixing

Many applications in aerospace engineering divulge that mixing is essential for efficient and effective jet performance. Jets are proficient in many engineering applications such as thrust vector control, thrust augmenting ejectors, high-powered gas lasers, and metal deposition. Jets are flowing from the nozzles of the missile; high-speed water jets are used for metal cutting. In air-breathing engines, efficient mixing is required to control combustion chamber size and enhance combustion efficiency to improve the aerospace vehicle range. For effective functioning of combustion cycles, mixing at small and large scales is desired. Small-scale mixing focuses on mixing at the molecular level, whereas large-scale mixing refers to large-scale vortices' breakup.

Since this region's formation is determined by the lateral degree of mixing occurring at the nozzle boundaries, the potential core's extent has been found to differ from the nozzle exit geometry (Sforza et al., 1966). The transition (Abramovich, 2020) or characteristic decay (Sforza et al., 1966) is sited forthwith downstream of the possible core region. The mixing introduced to the centerline velocity is achieved in this area, resulting in a smooth velocity profile with a dramatic decay in the jet (Namer & Otugen, 1988). Thereby, the coherent structures developed near the jet's boundaries control the jet's initial development (Namer & Otugen, 1988; Roshko, 1976). The velocity profiles achieve similarity in the axi-symmetric decay field (Sforza et al., 1966).

So, in general, the jet structure is divided into two regions: underdeveloped (comprising the potential core region and transition zone) and fully developed. Large-scale structured and small-scale irregular motions characterize the developing and developed regions of the jet, respectively. Furthermore, coherent systems are large-scale structured motions responsible for mass transport without being highly intense themselves. In comparison, small-scale structures known as incoherent structures are in charge of mixing promotion (Roshko, 1976). The dynamics of all free shear flows are regulated by large-scale coherent structures, which were discovered to play a significant role in the entrainment and mixing cycle (Brown & Roshko, 1974). As a result of the pairing phase, the initial vortices that form in the shear layer are convected downstream (Winant & Browand, 1974). This would result in a broader jet spread and a lower vortex frequency (Dimotakis & Brown, 1976). In jet shear layers, bulk mixing is controlled by large-scale coherent structures, while small-scale mixing is governed by turbulent velocity fluctuations (Brown & Roshko, 1974).

A supersonic jet varies fundamentally from its subsonic equivalent in structure. The degree of expansion, on the other hand, defines the structure of a supersonic jet. The potential core is no longer valid due to the shock-cell structure close to the nozzle exit. Because of waves in supersonic jets, the centerline velocity is not stable inside the core. As a result, it becomes challenging to identify the end of the core and measure its length in such jets. Accordingly, another variable known as the supersonic core length is being used to characterize jet mixing. The axial distance from the nozzle exit at which supersonic flow prevails is defined as the supersonic core length. (Anjaneyulu Krothapalli et al., 1990; Phalnikar et al., 2008; E. Rathakrishnan, 2010; Scroggs & Settles, 1996). The remaining areas of the jet are comparable to those of a subsonic jet, except where compressibility dominates the flow.

1.1.3 Development of Axi-symmetric Supersonic Jets

A supersonic jet flow is generally defined by similarity factors such as the static pressure ratio, $n = P_e/P_a$, the Mach number at the nozzle exit M , and the angle of inclination at the exit of the nozzle contour (Ginevskii et al., 2004). Previous research by (Bogdanoff, 1983; Dimitri Papamoschou & Roshko, 1988) has shown that compressibility effects minimize the growth rate of the shear layer. As a result, the shear layer in supersonic jets grows slower, affecting the jet production process. There are three potential expansion regimes in supersonic flow (see Figure 1.3), Where P_a (ambient pressure = P_b (back pressure)).

- $n = 1$ corresponds to the correctly expansion ($P_e = P_a$).
- $n < 1$ corresponds to the overexpansion ($P_e < P_a$).
- $n > 1$ corresponds to the underexpansion ($P_e > P_a$).

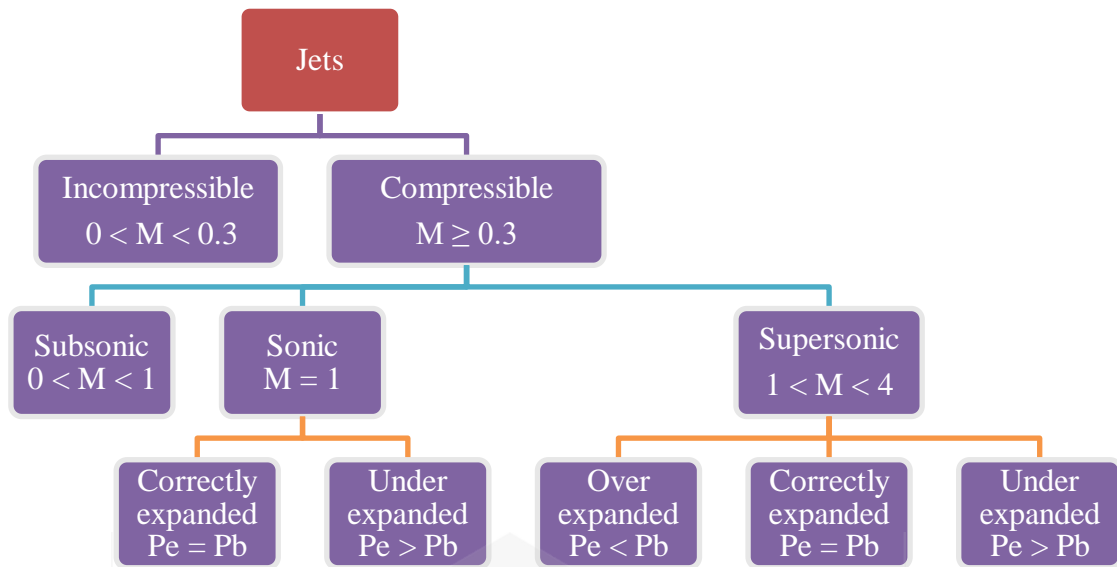


Figure 1.3 Classification of jets (E. Rathakrishnan, 2010)

The compressibility effect is quantified by the convective Mach number (M_c) (Bogdanoff, 1983; D. Papamoschou & Roshko, 1986). Unlike in subsonic jets, the influence of compressibility on mixing becomes important in supersonic planar, axisymmetric, and non-circular shear layers, leading to the impact of velocity and density gradients. As $M_c > 0.6$, the spreading rate of a plane shear layer falls precipitously to around 20% of the incompressible spreading rate (Chinzei et al., 1986; Clemens & Mungal, 1992; D. Papamoschou & Roshko, 1986). At moderately high Reynolds numbers, the shear-layer growth and entrainment in axi-symmetric jet configurations are dominated by the evolution of circular, azimuthally coherent vortex rings and their progressive merging (Crow & Champagne, 1971). Elliptic and rectangular jets have considerably higher entrainment levels than circular or two-dimensional jets due to vortex self-induction effects (Ho & Gutmark, 1987; H. S. Husain & Hussain, 1983; Hussain & Husain, 1989). Three-dimensionality emerges as a critical function of the jet structure at a short distance downstream of the jet exit, and streamwise vorticity dominates in entraining fluid from the surroundings (Liepmann